Superior imaging resolution in scanning helium-ion microscopy: A look at beam-sample interactions

David Cohen-Tanugi and Nan Yao[a)]
Princeton Institute for the Science and Technology of Materials, Princeton University, New Jersey 08544, USA

(Received 12 March 2008; accepted 15 July 2008; published online 16 September 2008)

Scanning helium-ion microscopy (SHIM) offers high-resolution imaging at the subnanometer scale. We employ Monte Carlo simulations to show the characteristics of the beam-sample interaction involved in SHIM, and compare it with those of scanning electron microscopy and scanning gallium-ion microscopy. We discuss the electronic and nuclear stopping powers and demonstrate that helium ions in matter possess a distinctive "electronic loss phase" in which inelastic collisions strongly dominate. This allows for large penetration depth, localized secondary electron emission, and high signal-to-noise ratio. We investigate the energy dependence of the interaction volume and show that for SHIM, spatial resolution can be further increased with energies beyond the customary 30 keV level. This paper provides a better understanding of the physics of SHIM and its conditions for high performance. © *2008 American Institute of Physics*. [DOI: 10.1063/1.2976299]

I. INTRODUCTION

In 2007, Carl Zeiss SMT announced a new imaging instrument which we call scanning helium-ion microscope (SHIM). Early investigations suggest that this technique can offer unprecedented image quality, even compared to the best existing scanning electron microscopy (SEM) or scanning gallium-ion microscopy (SGIM) instruments.[1,2] Because SHIM shows such high-level imaging capabilities for physical examination of materials, it is becoming crucial to have a a comprehensive understanding in its image formation mechanisms.

Imaging techniques that employ a focused charged particle beam to interact with a sample have been developed significantly since the 1960s.[3] The principles behind the beam-sample interaction that occurs when a particle beam is focused onto a material sample have been widely studied,[4,5] especially for electron beams (see Refs. 6 and 7 for a good summary of the beam-sample interaction of electrons). The works of Lindhard[8] and more recently Ziegler[9–11] have produced a useful framework for the study of beam-sample interactions for ions.

Before SHIM technology was officially released, its developers presented the new promises of this microscope. Notte *et al.* pointed out specifically the high brightness of the SHIM ion source, its high secondary electron (SE) yield, as well as the deep penetration of He^+ ions.[2,12] In July 2007, Inai *et al.* confirmed using Monte Carlo simulations that for helium-ion bombardment, the calculated SE yield of SHIM is much higher and the interaction volume is much narrower than that for SEM and SGIM. They suggested that "the spatial image resolution of SHIM with energies between 10 and 50 keV should be better ($\leqslant$0.1 nm) than for 30 keV Ga ion and 1 keV electron beams."[1] However, studies thus far have not placed sufficient emphasis on the reasons for such behavior or on the energy dependence of SHIM resolution. In this paper, we address these questions through a deep look at beam-sample interactions.

A. Background of beam-sample interaction for SHIM/SEM/SGIM

SHIM, SEM, and SGIM are scanning techniques whose main purposes are to provide high-quality imaging and analysis for materials. Their principles of operation are very similar: a beam of particles (electrons for SEM and ions for SHIM and SGIM) is focused on a point of the sample under observation and then sequentially scanned across the entire surface. As the beam particles penetrate the sample, they interact with the sample's atoms in a complex way that results in multiple collisions and the excitation of electrons, photons, etc.

The total region in which the beam interacts inside the solid is called the interaction volume. At each position of the beam, or pixel, detectors from the imaging device measure the number of particles that escape from the sample during the beam-sample interaction, and the pixel is assigned a grayscale value determined by the number of escaping particles detected. Generally, the detectors measure the output of SEs that originally belonged to the sample and escaped from the solid surface during the beam's excitation. Some imaging methods measure other forms of output such as backscattered ions, backscattered electrons, Auger electrons, X-rays, cathodoluminescence, etc., but this paper will focus on imaging using SE detection since it is the most relevant and useful technique in many cases.

B. Limiting factors in imaging resolution and contrast

Aside from the properties of the beam source and the incoming beam itself, one of the essential factors for final imaging quality is the yield of SEs that escape from the solid. The SE yield, δ, is an important factor because it determines the image contrast. During imaging, the brightness

[a)]Electronic mail: nyao@princeton.edu.

at each pixel is determined by the number of SEs detected while the beam was positioned at the corresponding location. Therefore, a relatively high SE yield allows for more subtle variations in topographic or material contrast in the final image. Even for a highly focused beam, spatial resolution is fundamentally limited by the distribution of escaping SEs. Here we define the interaction radius R as the radius inside of which SEs escape the solid, centered at the position of the incident beam.[13] Generally speaking, R is significantly larger than the radius of the incoming beam, so R offers a good estimate of the imaging resolution for an ideal zero-diameter beam.

Statistically, an ion collides multiple times within the solid but it generates at most one SE during each collision.[14] When a SE is generated, it typically travels until it encounters another atom and excites it with a fraction of its energy, liberating another SE which in turn continues this electron cascade. The original SE excited by the incoming beam has relatively high energy (50–100 eV), but this energy is then divided among all the SEs involved in the electron cascade, so only the electron cascades originating very close to the sample's surface are able to maintain enough energy to pass the surface potential barrier (of the order of 1 eV in most solids) and escape from the sample for detection.[7,9] More precisely, the yield of SEs produced at a depth z beneath the surface is proportional to $\exp(-z/D_e)$, where D_e is an "escape depth" of the order of 5–15 nm for most solids.[6,15] Therefore, SE detection is primarily a surface imaging technique, and the interactions below the escape depth of the solid are of little relevance for spatial resolution.

As numerous SEs leave the sample in the process of imaging, the net charge of the sample is altered. If the sample is an insulator, SEM and SGIM may therefore lead to important charging effects in the sample as charge builds up on the surface. Charging not only produces damage in the sample but it also affects imaging quality. Indeed, the presence of a strong accumulated electric charge can deflect the trajectory of the incoming beam as well as disturb escaping SEs. The local accumulation of surface charge thus limits the resolution and can produce serious imaging artifacts. The charging effect can be effectively mitigated using various methods for SEM and SGIM.[16,17]

A high signal-to-noise (S/N) ratio for emitted SEs is also important for high-quality image acquisition. A statistical approach to SE emission gives a S/N ratio of $[I_p/2e\Delta f(1+b)]^{1/2}$, where I_p is the probe current, Δf is the detector bandwidth, and $b \approx 1/\delta$ is the noise factor associated with SE yield δ.[18] SHIM currently uses an Everhart–Thornley detector: this detector setup is also widely used in SEM and SGIM systems, and its bandwidth is roughly 10 MHz.[2] Since I_p and Δf have comparable magnitudes for SHIM, SEM, and SGIM, the S/N ratio of each technique is primarily a function of the SE yield δ. The SE yield of SHIM has been observed to be relatively high [$\delta \approx 7$,[12] compared with $\delta \approx 0.1$ for SEM (Ref. 7)] so the theoretical S/N ratio of SEs in SHIM is significantly higher than equivalent SEM acquisitions. Further research would be needed for more precise considerations regarding the S/N ratio of SHIM.

The SE yield, the interaction radius, and the possibility of charge accumulation are important factors in image acquisition. Hereafter, we discuss the natural advantages and/or disadvantages that SHIM possesses with respect to these various factors by examining the process of beam-sample interaction for a typical He^+ ion beam and comparing it with equivalent Ga^+ ion and electron beams.

II. DESCRIPTION OF SHIM INTERACTION

A. A typical SHIM beam-sample interaction

An important contribution made by Bohr to the study of ion interactions in matter is the idea that the collisions between ions and sample atoms can be statistically treated as two independent types of events: electronic collisions and nuclear collisions.[14] In an electronic collision, the ion is said to scatter inelastically from the atom, exciting a SE in the sample atom and losing energy in the process, but maintaining its original direction since its mass is much larger than the electron mass. The electron mass is 9.1×10^{-31} kg, while the masses of He^+ and Ga^+ are 6.64×10^{-27} and 1.15×10^{-25} kg, respectively, or 7000 times and 126 000 times more than an electron. In a nuclear collision, the ion scatters elastically without exciting any electrons.

As the He^+ beam enters the solid with high energy, it experiences mainly electronic collisions, generating multiple SEs along the way and gradually losing kinetic energy. Since we can treat electronic collisions as purely inelastic, the beam maintains its direction quasi-perfectly without scattering. We call this stage of the interaction the "electronic loss phase" and define the electronic depth L as the characteristic depth traveled by the beam before nuclear collisions become significant, i.e., the average depth of the electronic loss phase.

As the ions lose energy, they enter a "nuclear loss phase:" nuclear collisions become increasingly frequent, and at a depth of order L the ions begin to experience predominantly nuclear collisions, thus scattering at increasingly large angles within the solid and broadening the interaction volume. Although the definition of L may suggest that the transition from electronic to nuclear loss phase is an abrupt one, it is, in fact, a gradual process and L indicates mainly the characteristic distance involved, much like a characteristic decay time describes an exponential decay. At each nuclear collision, the ion transfers a fraction of its energy to the target atom. If the incident particle has energy E and it transfers an energy T to the target atom, the fraction is found from classical mechanics to be

$$\frac{T}{E} = \left(\frac{4M_1M_2}{(M_1+M_2)^2} \right) \sin^2(\theta/2),$$

where M_1 is the mass of the projectile, M_2 is the mass of the target atom, and θ is the ion's scattering angle.[4] If T is smaller than the lattice binding energy, E_{binding}, of the solid (15–25 eV), then the target atom remains bound at its position inside the solid and the energy is converted into phonons in the sample. However, if $T > E_{\text{binding}}$, the target atom is recoiled out of its lattice position and may initiate a collision cascade by colliding with other atoms in the sample.[10] Just

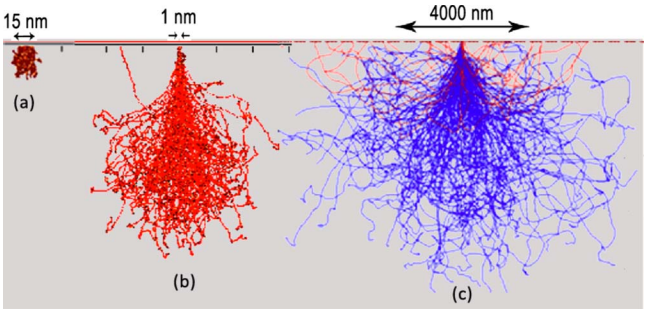

FIG. 1. (Color online) Comparison of interaction volumes for SHIM (center), SGIM (left), and SEM (right) in a Si sample. The interaction volume of SHIM is sharply peaked at the incoming point, allowing for a significantly smaller interaction radius than SGIM or SEM. In all three cases, the beam enters at the top of the figure and is simulated with zero width and $E=30$ keV. (The SEM result is not to scale because of its significantly larger interaction volume.)

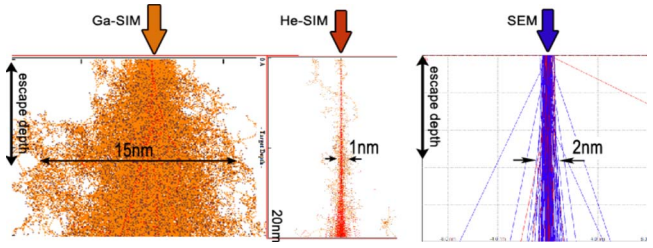

FIG. 2. (Color online) Same comparison as Fig. 1, with a zoom on the first 20 nm of the sample. The escape depth is taken to be approximately 10 nm, and for each beam the radius of interaction is measured as the maximum width attained above the escape depth.

like incoming ions, recoiled atoms may also generate SEs during collision cascades, so collision cascades are an important factor in the interaction volume and for the interaction radius R (this is discussed in Sec. II C below). However, helium has relatively small mass ($A=4$) compared to typical sample elements, which can range from light solids such as carbon ($A=12$) to heavy solids such as lead ($A=207$). Consequently, He^+ ions can only confer small velocities to sample atoms compared to their own initial velocity, and collision cascades are not a large effect for SHIM. Let us consider a typical SHIM apparatus, with energy $E=30$ keV, a small beam diameter (<1 nm), and a reasonable beam current of about 10 pA.[12] When the helium ions enter the sample, they have relatively large energy (30 keV, i.e., $v \approx 1.2\times10^6$ m/s). To begin, they interact mainly with the sample electrons, losing energy along the way but maintaining their overall direction. After a sequence of nuclear collisions, each helium ion has lost enough energy that it cannot excite anymore atoms; if it has not been backscattered away from the solid at some point during the interaction, it eventually comes to a stop and remains within the solid.

B. Visualization and comparison with SEM and SGIM

Section II A summarized the qualitative behavior of a helium-ion beam in a solid. Here we provide an illustration to this process based on the simulations using the SRIM software package developed by Ziegler.[19] Figure 1 shows a typical cross section of a beam-sample interaction for a helium-ion beam, in comparison with interactions for a gallium-ion beam and an electron beam of the same beam diameter $d=0$ at 30 keV. The interaction volume of the SHIM beam in Fig. 1(b) is "thin" and localized for the first few dozens of nanometers before it begins to broaden due to nuclear collisions, as described above. Here L is larger that the escape depth, D_e, so the spatial resolution is not limited substantially by the interaction volume. In comparison, the SGIM interaction volume [Fig. 1(a)] is never truly localized; it broadens immediately upon entering the solid, so we may say that here $L\rightarrow0$. Furthermore for SEM at 30 keV in Fig. 1(c), the electrons penetrate and scatter far more easily than either helium or gallium ions, and their interaction radius is therefore much larger. Due to their small mass relative to target atoms, projectile electrons may collide elastically with target nuclei, but they do not collide inelastically within the sample in the same way that ions do. Therefore, projectile electrons from a SEM beam do not experience "electronic collisions" with sample electrons in the sense introduced by Bohr. Therefore, the notion of "electronic depth" L is not well defined for SEM, and projectile electrons quickly scatter from their initial direction upon entering the sample.

Figure 2 shows the same interaction volumes as Fig. 1, but with a zoom only on the escape depth just below the sample's surface. In this figure, all three results are to scale, and it appears even more clearly that while SGIM has a very large interaction radius (15 nm), the interaction radius of SHIM is smaller than 1 nm. As for SEM, the interaction volume is highly peaked in a diameter of about 2 nm; although this interaction radius is only slightly larger than that of SHIM, the full interaction in Fig. 1 shows that there is nevertheless a certain amount of SE excitation occurring outside these few nanometers. These SEs are often classified as SE2, and they contribute to decreasing the effective spatial resolution for SEM.

Unlike SEM, scanning ion microscopy techniques that use positive ions are especially at risk of producing undesirable charging effects since both the incoming ions and the escaping SEs contribute positive charge to the sample. Given the reported high SE yield of SHIM and its highly localized interaction radius, one may fear that the spatial resolution of SHIM, and accordingly its image quality, will be significantly hindered by strong charging effects. A quick calculation indicates that in the operating conditions described by the developers,[1] with a SE yield $\delta=7$ and $I=10$ pA, the sample will accumulate a charge as large as $Q\approx Q_+-Q_-=8\times10^{-12}$ C/s, where Q_+ is the positive charge accumulated from stopped ions and Q_- is the negative charge escaping from the solid, neglecting backscattered ions and second-order effects. This calculated charge accumulation indeed represents a problem for SHIM imaging of insulators since SEs can only escape from the surface region where accumulated charge may perturb their trajectory. Regarding the incoming He^+ ions, however, Fig. 1 shows that they become buried inside deep regions of the sample (>100 nm), so their contribution to charge accumulation is actually well below the surface and far too deep to significantly affect the imaging acquisition. Thus, the insulating nature of a sample may actually play in its favor when it comes to partially reducing

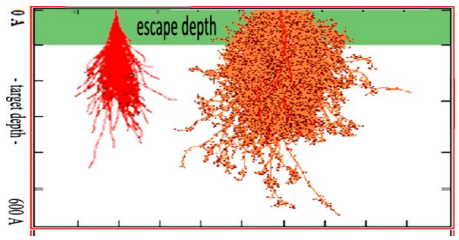

FIG. 3. (Color online) Simulation of ion distribution (left) vs full collision cascades due to recoiled sample atoms (right) for Ga^+ ions in silicon at $E=30$ keV. Although the incoming ions penetrate the solid with little scattering, recoiled atoms inside the sample lead to a broad interaction radius.

the extent of charging during SHIM imaging. Fortunately, charging effects can also be significantly reduced by using an *in-situ* electron flood gun to neutralize surface charge between image scans.[20]

C. Collision cascades

In effect, SE generation is not limited to collisions of projectile ions with sample atoms; recoiled sample atoms and high-energy electrons generated by the primary beam may also create collision cascades. For SGIM, the actual interacting volume is dominated by the effect of collision cascades due to recoiled sample atoms. This is apparent in Fig. 3: the interaction volume of the Ga^+ ions themselves (left in Fig. 3) is not fundamentally different in shape from that of He^+ (left in Fig. 4). However, when the simulation takes into account the collision cascades associated with each nuclear collision (right in Fig. 3), it becomes clear that a SGIM beam generates collision cascades as soon as it enters the sample—there exists no electronic loss phase at any reasonable beam energy for Ga^+ ions because nuclear collisions are always dominant.

In contrast, the equivalent simulations for SHIM (right in Fig. 4) indicate that the collision cascades initiated by He^+ ions are far less numerous than for Ga^+. The effect of collision cascades due to recoiled atoms only broadens the interaction volume of SHIM by 5%–15% compared to the trajectory of incoming ions, allowing for a more localized interaction volume than for SGIM.

When high-energy SEs (SE1) are generated by the incoming beam, they can also create electron cascades which liberate low-energy SEs (SE2) in a broad area around the beam position, much like collision cascades due to recoiled atoms. In SEM, incident electrons cannot transfer significant momentum to target atoms because of their comparatively small mass. Therefore, the relative contribution of electron cascades to the SE generation process in SEM is high.[7] In SHIM and SGIM, however, the contribution to SE generations due to electron cascades is marginal compared to contributions due to the incident beam and to recoiled sample atoms. Indeed, even high-energy SEs have energies below 50 eV,[18] whereas incident ions and recoiled atoms have energies in the keV range, and thus initiate far more energetic cascades that dominate the SE generation process. For this reason, the Monte Carlo simulations for SHIM and SGIM represented in Figs. 3 and 4 do not take into account the marginal effect of electron cascades. The theoretical discussion in the following paragraph will account for these observed behaviors.

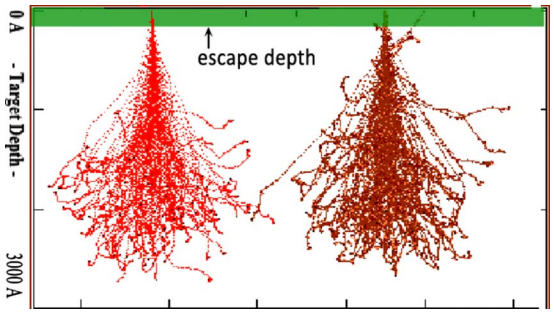

FIG. 4. (Color online) Simulation of ion distribution (left) vs full collision cascades due to recoiled sample atoms (right) for He^+ ions in silicon at $E=30$ keV. Collision cascades have little effect on the shape of the interaction volume.

III. A THEORETICAL EXPLANATION

A. Electronic and nuclear stopping power

Although there exists no closed form expression to describe the average interaction of a projectile ion or electron with matter, the trajectory of projectiles inside a solid is well described in terms of the stopping power S, which is defined as the energy lost per distance traveled: $S=-dE/dx$.

The stopping powers arising from electronic and nuclear collisions, denoted S_e and S_n, respectively, can be treated as independent in the description of Bohr.[14] For a given ion and a given sample material S_e and S_n depend largely on the energy of the ions. For simplicity we restrict our discussion to a single sample element, chosen arbitrarily to be Al (the interaction dependence on the sample material is described in Refs. 21 and 22). In the high-energy limit, nuclear collisions are very small [less than 0.1% of dE/dx (Ref. 10)] and the stopping power is given by the classical Bethe–Bloch formula

$$S_e = 4\pi Z_2 \frac{Z_1^2 e^4}{mv^2} \ln\left(\frac{mv_b^3}{Z_1 e^2 \omega}\right),$$

where v_b is the Bohr velocity and ω is the orbital frequency (see Ref. 11 for a more complete discussion of high-velocity stopping power theories). Since the Born approximation is only valid when the scattered amplitude is significantly smaller than the transmitted amplitude, this formula is accurate only at relatively high energies ($E>5$ MeV) and when nuclear charge and nuclear energy loss are not taken into account.[11] In the low-energy range, Bethe–Bloch theory becomes inaccurate because the incoming ion is likely to become neutralized by capturing a sample electron. In this case the nuclear stopping power begins to dominate, and the LSS equation derived by Lindhard, Scharff, and Schiott gives an expression for S_e and S_n, and the electronic stopping power takes the form

$$-(d\varepsilon/d\rho)_e = \kappa\varepsilon^{1/2},$$

with dimensionless units of energy ε and distance ρ.[8] The expression for S_n is obtained via the scattering differential cross section $d\sigma/d\Omega$ of an ion from a target using the

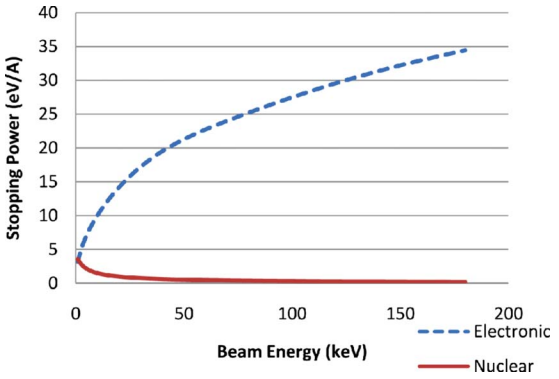

FIG. 5. (Color online) Energy dependence of S_e and S_n for helium ions in Al. For beam energies above 10 keV, S_e is larger than S_n by at least one order of magnitude.

Thomas–Fermi atomic model.[5,14] Based on these models and on experimental data, the energy dependence of electronic and nuclear stopping power for any ion and sample material is given by Ziegler in SRIM. These stopping powers are obtained primarily by scaling the stopping powers of hydrogen, using an empirical ion effective charge Z_1^* and an empirical scaling factor.[11] Figure 5 shows the calculated values for He^+ ions in aluminum using SRIM.

Figure 5 indicates that if the helium-ion beam begins with energy $E>20$ keV, the nuclear stopping power is negligible compared to the electronic stopping power ($S_e/S_n>20$). As the incoming ions lose their energy in the solid, they travel gradually leftward along the curve until they reach the region of very low energies ($E<3$ keV) at which S_n become significant. This closely confirms what was stated earlier: namely, that the SHIM beam enters the solid with barely any nuclear collisions, and only after having lost much energy in electronic collisions and having traveled beyond a non-negligible depth L do the helium ions finally begin to collide elastically and truly scatter in the sample. Therefore, the energy dependence of stopping powers for helium explains the characteristic interaction for SHIM described above and the results of our simulations.

This energy dependence also suggests another notable characteristic of SHIM. In the LSS regime, S_e increases quadratically with ion energy until E reaches the Fermi energy and continues to increase monotonically with energy for $E \leqslant 500$ keV for helium. As the incoming SHIM energy is increased to 50 or even 150 keV, the electronic depth L becomes even greater. Since the escape depth D_e is fixed for a given sample, the interaction radius—and accordingly, the imaging resolution—can actually be optimized significantly by increasing the incident beam energy: R is reduced by roughly 40%–50% if the energy is doubled from 30 to 60 keV. This is confirmed by Monte Carlo simulations such as Fig. 6, which shows the cross-sectional interaction volumes of a He^+ beam for various energies. Although the penetration depth increases for large beam energy, the interaction radius of SHIM decreases as E is raised. Moreover, the results in Fig. 5 also indicate that the SE yield should also increase with incident He^+ beam energy as a consequence of increasing electronic stopping power. The increase SE yield represents yet another factor in favor of high-energy operation of SHIM.[1]

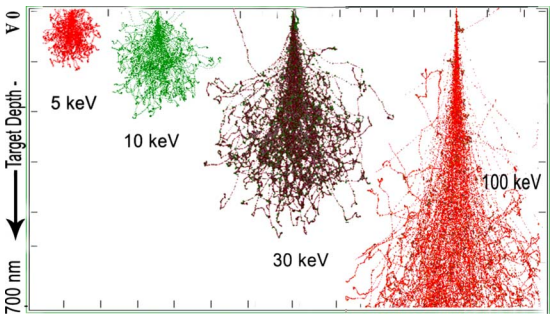

FIG. 6. (Color online) Interaction volume of SHIM in Si for E=5, 10, 30, and 100 keV. As E is increased, the penetration depth increases but the interaction radius R becomes smaller.

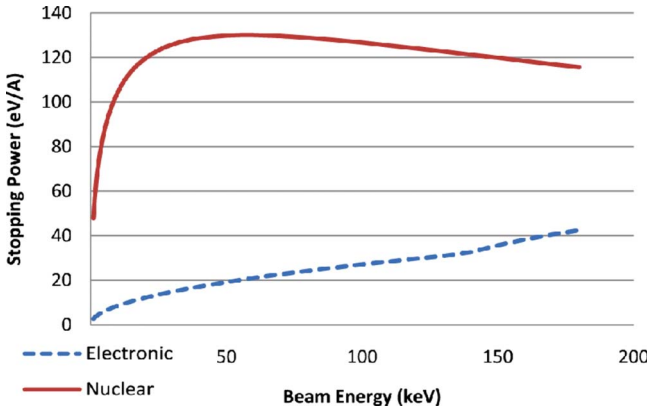

FIG. 7. (Color online) Energy dependence of S_e and S_n for gallium ions in Al. Even for low beam energies, S_n dominates the interaction process.

The opposite trend holds for electrons and gallium ions in most solids. For SGIM operating between 0 and 50 keV, Fig. 7 shows that S_n actually *increases* as the beam energy is increased, so high beam energy does not solve the problem of large interaction radius at all. In fact, even for small energies of the order of 1 keV, the graph indicates that $S_e \ll S_n$. Physically, the dominant effect of nuclear collisions is essentially due to the large mass of gallium (A=70), which is demonstrated by the fact that for a fixed energy (say, 30 keV) the ratio S_n/S_e rapidly exceeds unity for ions with atomic number as low as Z=8 (see Fig. 8). The interaction only

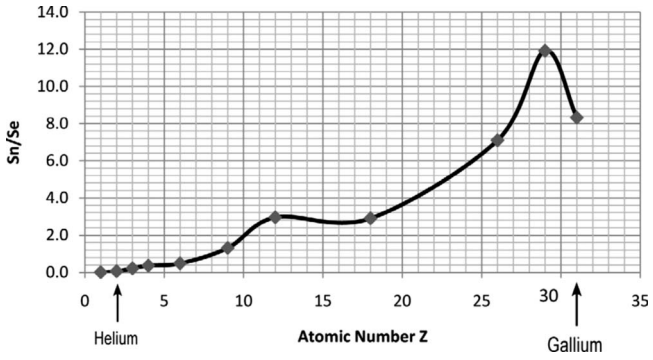

FIG. 8. Ratio of S_n/S_e in Plexiglas as a function of ion atomic number onto an AL sample, taken at E=30 keV. The ratio is only smaller than unity for very light ions such as He^+ (data reference: ion stopping and table ranges, SRIM).

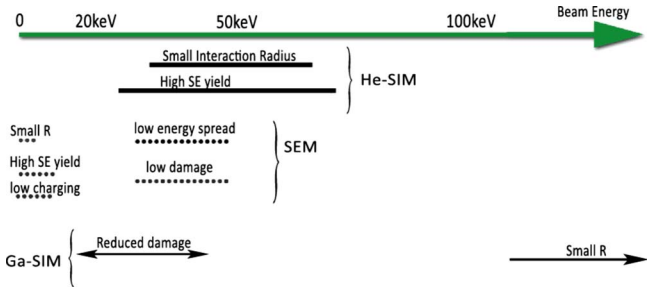

FIG. 9. (Color online) Optimal energy ranges for various factors in imaging quality for SHIM, SEM, and SGIM. The various advantages and drawbacks of low-energy SEM are described in Ref. 7, while the energy-dependent image quality for SGIM are detailed in Refs. 4 and 14.

begins with a distinct electronic loss phase for very light ions such as He^+.

Numerically, the change of regime between low energy (described by the LSS equation) and high energy (described by Bethe theory) occurs at the order of $E=v_bZ^{2/3}$, where $v_b=2.19\times10^7$ m/s is the Bohr velocity.[8] Thus for gallium, S_e increases linearly with v for any energy below $E=1.75$ GeV—but at such a high energy a SGIM beam would completely destroy the sample. Therefore, in contrast to SHIM, gallium has the distinct disadvantage that collision cascades within the SE escape depth dominate the interaction volume for any reasonable beam energy.

In respect to electrons, the ratio $A=M_{\text{target}}/M_{\text{projectile}}$ is extremely large, so electrons virtually lose no energy when they scatter from nuclei even at large angles θ. Therefore, electrons interacting in a sample conserve their kinetic energy much longer than ions and travel, on average, much further than ions. This provides a basic explanation for why the SEM beam (Fig. 1) has such a large interaction volume. Albeit with a different terminology, Joy showed that the "interaction radius" of a SEM beam broadens for increasing energy, much like SGIM.[6,7] Since R is optimized for low energy and the SE yield of electrons increases with low energy as well, SEM instruments are often operated at a low-energy regime of the order of 1 keV. However, the interaction radius remains wider for SEM than for SHIM even for low-energy incident electron beam.[2]

B. Comparison of energy ranges

For SHIM, SGIM, and SEM imaging, the incident beam energy has a large influence on the factors that control the imaging quality such as incident beam diameter, interaction radius, SE yield, sample charging, beam damage, etc. Each imaging technique possesses its own optimal energy range or possibly several different energy ranges depending on the priorities of a given experiment. Figure 9 summarizes qualitatively the different energy ranges that optimize these different factors in imaging quality for SHIM, SEM, and SGIM. As shown above, SHIM displays the notable property that most factors in its imaging quality are simultaneously optimized at high energies. In contrast, these optimizing energy ranges do not coincide for SEM and SGIM. For SEM, the very-low-energy range ($\approx$1 keV) optimizes interaction radius and SE yield, but only at higher energies can low damage and low energy spread be achieved. For SGIM, only impractical energies (sufficient to locally destroy the sample) can minimize the interaction radius, as argued herein. With SHIM it appears that the dilemma of which energy range to use is mostly solved: the factors in imaging quality all coincide in the same energy range.

The present discussion was mainly restricted to the factors in imaging resolution that relate to beam-sample interaction, so we made the simplification that beam current, focusing precision, energy spread, signal collection efficiency, and other "external" factors could be taken as constant; clearly this simplification has its limitations. Nevertheless, the present arguments provide a valuable qualitative description of energy optimization of factors in beam-sample interaction.

IV. CONCLUSION

Our study presents evidence showing that SHIM possesses a narrower interaction radius than existing SEM and SRIM, and thus offers higher spatial imaging resolution. The imaging resolution is largely limited by the interaction radius of the acquisition, which is in turn determined by the incident beam energy, the distribution of electronic and nuclear stopping powers, and the extent of collision cascades. Being both lighter than most sample nuclei and much heavier than electrons, He^+ ions penetrate with weak scattering and initially experience an electronic loss phase in which the beam is only weakly scattered. This results in small interaction radius and high SE yield. At energies above 25 keV, the spatial resolution of SHIM ceases to be limited by the interaction radius, which is of the order of 1 nm. Therefore, the spatial resolution of SHIM imaging can be further reduced for energies between 30 and 70 keV. Although SEM and SGIM technologies can often be operated at low energies (below 5 keV), there is little interest in low-energy SHIM for imaging since the interaction radius increases and the SE yield decreases for these low-energy ranges.

One important question that remains to be answered on this topic is the effect of sample charging. The amount of charging may be especially worth worrying about if the SE yield of SHIM is as high as 7 or 8.[1] Even if the ions themselves are deeply buried within the sample, the high rate of escaping SEs may still lead to undesirable charging effects. However, SHIM can be made less susceptible to these charging effects at high energies since projectiles with high energy are less scattered by a charged potential. This may provide a significant advantage for imaging both soft and nanoscaled materials. SHIM technology represents a substantial advance in the field of high-resolution microscopy, and we expect it will offer a variety of new applications.

ACKNOWLEDGMENTS

This work was partially supported by the National Science Foundation-MRSEC program and the New Jersey Commission of Science and Technology.

[1] K. Inai, K. Ohya, and T. Ishitani, J. Electron Microsc. **56**, 163 (2007).
[2] J. Notte, B. Ward, and N. Economou, AIP Conf. Proc. **931**, 489 (2007).
[3] D. McMullan, *51st Annual Meeting of the Microscopy Society of America*

(Cambridge University, Cincinnati, OH, 1993).
[4]N. Yao, *Focused Ion Beam Systems: Basics and Applications* (Cambridge University Press, Cambridge, 2007).
[5]J. Orloff, L. Swanson, and M. W. Utlaut, *High Resolution Focused Ion Beams: FIB and Its Applications: The Physics of Liquid Metal Ion Sources and Ion Optics and Their Application to Focused Ion Beam Technology* (Kluwer Academic, New York, 2003).
[6]D. C. Joy and C. S. Joy, Micron **27**, 247 (1996).
[7]D. C. Joy and J. B. Pawley, Ultramicroscopy **47**, 80 (1992).
[8]J. Lindhard, Proc. R. Soc. London, Ser. A **311**, 11 (1969).
[9]J. F. Ziegler, J. Appl. Phys. **85**, 1249 (1999).
[10]J. F. Ziegler, J. P. Biersack, and U. Littmark, *The Stopping and Range of Ions in Solids* (Pergamon, New York, 1985), Vol. 1.
[11]J. F. Ziegler, J. P. Biersack, and M. D. Ziegler, *SRIM, the Stopping and Range of Ions in Matter* (SRIM Co., Chester, MD, 2008).
[12]J. Morgan, J. Notte, P. Hill, and B. Ward, Microscopy Today **14**, 24 (2006).
[13]Inai *et al.* define more formally an analogous quantity as "the lateral distance for which the cumulative probability of SE generation is 0.5."
[14]M. A. Nastasi, J. K. Hirvonen, and J. W. Mayer, *Ion Solid Interactions: Fundamentals and Applications* (Cambridge University Press, Cambridge, 1996).
[15]N. Yao, C. Harrison, D. H. Adamson, M. Park, P. Chaikin, and R. A. Register, Microsc. Microanal. **3**, Suppl. 2, 1241 (1997).
[16]M. A. Stevens-Kalceff and K. J. Levick, Microsc. Microanal. **10**, 1116 (2004).
[17]B. L. Thiel and M. Toth, J. Appl. Phys. **97**, 051101 (2005).
[18]L. Reimer, *Scanning Electron Microscopy: Physics of Image Formation and Microanalysis* (Springer, Berlin, 1998).
[19]The CASINO software was used for SEM simulation, while SHIM and SGIM results were obtained using the SRIM 2006 (stopping range of ions in matter) software developed by Ziegler (see www.gel.usherbrooke.ca/casino and www.srim.org). SRIM calculates the trajectory of ions into matter based on statistical descriptions of ion stopping and range, obtained for He+ by direct measurements as well as by scaling the stopping powers of hydrogen using an empirical ion effective charge Z^{1*} and an empirical scaling factor.
[20]H. L. Richard, G. Yuval, L. Ted, and G. Michael, J. Vac. Sci. Technol. B **25**, 2547 (2007).
[21]K. Ohya, Nucl. Instrum. Methods Phys. Res. B **206**, 52 (2003).
[22]K. Ohya and T. Ishitani, Surf. Coat. Technol. **158–159**, 8 (2002).